International Journal of Infrared and Millimeter Waves
https://doi.org/10.1007/s10762-018-0556-5

Complex Permittivity Measurement of Paraffin Phase-Change Material at 26 GHz–1.1 THz Using Time-Domain Spectroscopy

Behnam Ghassemiparvin[1] · **Nima Ghalichechian**[1]

Received: 27 July 2018 / Accepted: 20 November 2018 / Published online: 29 November 2018

Abstract

We report complex permittivity measurement of hexatriacontane films at the frequency range of 26 GHz–1.1 THz. Hexatriacontane ($C_{36}H_{74}$) has a melting point of 75 °C that exhibits a 15% volumetric change which is crucial in developing low-loss RF microactuators with large displacement. In this work, we employ time-domain spectroscopy to measure the transmission coefficient of the paraffin samples in the frequency range of 0.3–1.1 THz. In order to extract the dielectric constant and accurately estimate the small values of loss tangent, we developed a propagation model which measured data are fitted to through a new least-squares minimization method. A Debye relaxation model is used to model the frequency dependence of the permittivity. Described method is rapidly convergent with minimum amount of signal processing. This method can be used to determine the complex permittivity of the materials by devising an appropriate function for the frequency dependence of the complex permittivity. Transmission through 20 samples of paraffin with various thicknesses is measured and the average permittivity is found to be 2.25 with standard deviation of 0.028. The loss tangent is monotonically increasing with frequency and the maximum value is 6.32×10^{-3} at 1.1 THz. Our study demonstrates that paraffin is a low-loss dielectric which makes it an attractive candidate for development of electro-thermo-mechanical actuators for sub-millimeter- and millimeter wave (mmW) variable capacitors, low-loss reconfigurable antennas, and phase shifters.

Keywords Alkane · Complex permittivity · Loss tangent · Millimeter wave · Paraffin · Terahertz · Time-domain spectroscopy

✉ Behnam Ghassemiparvin
ghassemiparvin.1@osu.edu

Nima Ghalichechian
ghalichechian.1@osu.edu

[1] Department of Electrical and Computer Engineering, Electroscience Laboratory, The Ohio State University, Columbus, OH 43212, USA

1 Introduction

Paraffin is a mechanical phase-change material that exhibits a 15% reversible volumetric change during its solid-liquid transition at relatively low temperatures (37–75 °C). Paraffins are class of normal alkanes (n-alkanes) which are the simplest isomers with straight chain. Alkanes have the chemical form of C_nH_{2n+2} where n is typically between 20–50. In addition, due to its nonpolar molecular structure, paraffin is expected to have a low dielectric loss at millimeter-wave (mmW) and terahertz (THz) bands. This unique combination of electrical and mechanical properties makes paraffin an attractive candidate for the development of a new class of electro-thermo-mechanical RF actuators [1, 2]. This novel type of RF actuators can be utilized in developing high-quality factor mmW variable capacitors, low-loss reconfigurable antennas, and phase shifters. Determining the capacitance and dielectric losses associated with these variable capacitors requires accurate measurement of the complex permittivity of paraffin. In addition, paraffin is used in embedding biological tissues—due to its superior tissue morphology preservation—in THz time-domain spectroscopy studies [3]; hence, determining the effect of paraffin layer requires accurate permittivity characterization.

Dielectric loss and relaxation of liquid n-alkanes ($n < 20$) were studied in [4–6] where resonator techniques and Fourier spectrometry are used in microwave and far infrared bands, respectively. Maximum loss tangent of 12×10^{-4} at the frequency range of 2–6 THz was reported for liquid alkanes, with $n < 14$. Laib et al. measured the dielectric properties of liquid n-alkanes using time-domain spectroscopy (TDS) in the frequency range of 0.1–2.5 THz and reported that the absorption coefficient of these nonpolar liquids has approximately a linear frequency dependence with no significant peaks [7]. In [8, 9], refractive index and absorption coefficient of solid paraffin waxes consisting of mixture of alkanes are studied. Paraffin waxes with melting points of less than 58° [8] and mixture of solid n-alkanes with $n < 31$ [9] has no significant absorption peaks in the frequency range of 0.2–2.5 THz, and increases monotonically with increasing frequency. However, measured values and extraction method used in [8, 9], which is based on single transmission and accurate knowledge of the thickness, are not accurate enough for RF design purposes. In addition, an analytical model is not presented to extrapolate the values for lower frequencies. Even though there are extensive studies on the dielectric loss of liquid n-alkanes, to the authors best knowledge, there is no measurement reported for the dielectric permittivity of the solid alkanes with carbon atoms of $n > 20$. Our preliminary study on the complex permittivity of hexatriacontane ($C_{36}H_{74}$) were presented in [10, 11].

TDS is a free-space measurement technique where material properties can be extracted for a wide frequency range. This is in contrast to the narrowband resonator-based measurement techniques [4]. In addition, since the measurements are carried out in the time domain, phase of the electric field is also measured. In TDS, temporal profile of the of transmitted electric field is measured with and without the sample. Ratio of the Fourier transform of these signals provide us with the phase and amplitude of the transmission coefficient as a function of frequency. Then, an inverse problem is solved to extract the complex permittivity of the sample [12]. A model-based extraction scheme is described in [12] where a complete knowledge of

the sample thickness is required to extract the complex refractive index. Uncertainties in the thickness of the sample could result in artificial oscillations in refractive index with respect to frequency. Precise determination of the thickness is also possible by considering the multiple reflections in the sample that can be temporally separated [13, 14]. An improved extraction algorithm is presented in [15] where the accuracy is enhanced by constructively using the uncertainty of the measurement. An extensive study on the model-based extraction of the complex permittivity using reflection-transmission mode spectroscopy is presented in [16] where no initial guess for the thickness is required.

In this work, we report the complex permittivity measurement of hexatriacontane ($C_{36}H_{74}$) films with melting point of 75 °C, using TDS. We developed a propagation model-based characterization scheme using the least-squares optimization. Propagation model considers the multiple internal reflections in the sample—Fabry-Pérot effect—for both thick and thin samples which increase the accuracy in measuring the loss tangent. Therefore, temporal windowing is not required for this method. Since the accuracy of the permittivity measurement depends on the precision of the sample thickness, effective thickness of the sample is also determined through the least-squares fitting process. A new error function based on the real and imaginary part of transmission coefficient is defined for accurate and rapid convergence of the optimization. Debye relaxation is used to model the complex permittivity of hexatriacontane which ensures its smooth variation with respect to the frequency. In addition, this method can be used to determine the complex permittivity of the materials by devising an appropriate function for the frequency dependence of the complex permittivity. To evaluate the performance of the extraction process, it is tested on large number of simulated cases with varying dielectric constant and loss tangent.

2 Description of the Complex Permittivity Extraction Method

To extract the complex permittivity of the sample, measured amplitude and phase of the transmittance are fitted to a three-layer plane wave propagation model where the sample is positioned between two layers of air as shown in Fig. 1a. A picture of our measurement setup is shown in Fig. 1b. We have made the following assumptions in our work:

1. Sample is a linear, isotropic, and homogeneous medium.
2. Sample has two flat and parallel surfaces with a thickness of d.
3. Plane wave is normally incident on the surface of the sample.

Note that, in a THz-TDS system, plane-wave transmission can be considered, if the sample thickness is much smaller than the depth of focus of the system. These underlying assumptions and associated errors are studied extensively in [16]. Considering these assumptions, the transmission coefficient through the sample is adopted from [17] as follows:

$$T = \frac{4k_0k_d \exp(-j(k_d - k_0)d)}{(k_d + k_0)^2 - (k_d - k_0)^2 \exp(-2jk_d d)}, \tag{1}$$

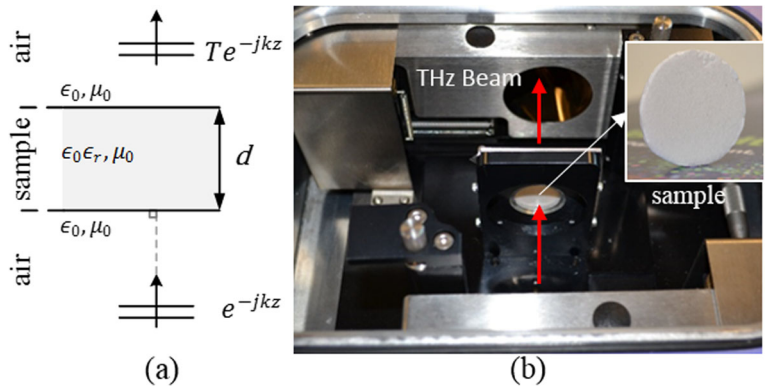

Fig. 1 **a** Three-layer propagation model with the normal incident plane wave, **b** view of the measurement chamber of the THz-TDS system and sample

where k_0 is the wave number in air and k_d is the complex propagation constant in sample defined as $k_d = k_0\sqrt{\epsilon_r}$. Note that transmission coefficient defined in Eq. 1 takes into the account the multiple internal reflections—Fabry-Pérot effect— in the sample. ϵ_r is the frequency-dependent relative complex permittivity of the sample, and it is modeled using Debye relaxation as follows:

$$\epsilon_r = 1 + \frac{\epsilon_s - 1}{1 + j\omega\tau}, \tag{2}$$

where τ and ϵ_s are relaxation time and the static permittivity, respectively, and determined using the least-squares fitting. Debye relaxation model ensures the smooth variation of real and imaginary permittivity with respect to the frequency.

In order to determine the unknown coefficients of ϵ_s, τ, and d, MATLAB's nonlinear least-squares solver is employed and the following error function is used,

$$\delta(\epsilon_s, \tau, d) = \delta_{\Re}^2 + \delta_{\Im}^2, \tag{3}$$

$$\delta_{\Re} = \ln(|T|^2)\cos\phi - \ln(|T_{\text{meas}}|^2)\cos\phi_{\text{meas}}, \tag{4}$$

$$\delta_{\Im} = \ln(|T|^2)\sin\phi - \ln(|T_{\text{meas}}|^2)\sin\phi_{\text{meas}}. \tag{5}$$

$|T|\angle\phi$ and $|T_{\text{meas}}|\angle\phi_{\text{meas}}$ are the modeled and measured transmission coefficients, respectively. $\delta_{\Re}$ and $\delta_{\Im}$ are related to the real and imaginary part of the transmission coefficient. Unlike the error functions defined in [12] and [14] where amplitude and phase are used, here we have used the real and imaginary part of the transmittance in our error function. Real and imaginary part of transmittance are both in the range of $(-1,1)$; hence, they have equal weight in $\delta(\epsilon_s, \tau, d)$. The error function is minimized in terms of least squares to extract the unknown parameters. Mechanical measurement of the sample thickness is used as the initial guess. Starting value for ϵ_s is determined by measuring the average frequency difference between the peaks of the transmission coefficient, Δf (discussed later on), as follows:

$$\epsilon_s^0 = \left(\frac{c}{2\pi}\right)^2 \frac{1}{(\Delta f d_0)^2}, \tag{6}$$

where d_0 is the initial guess for thickness and c is the speed of light in vacuum. Once the relaxation model parameters are extracted, real permittivity and the loss tangent are calculated using Eq. 2.

To evaluate the performance of the extraction method, transmission through samples with various thickness and permittivity is simulated in ANSYS HFSS. The simulated transmission coefficient is used to extract the complex permittivity. Thickness of the simulated sample is varied as 0.4–2 mm with steps of 0.4 mm and its static permittivity and relaxation time are varied as $2.15 < \epsilon_s < 2.3$ and $0.5 < \tau < 2$ fs. Initial guess for τ is set to 0.01 fs, and a uniformly distributed error with a standard deviation of 0.15 mm is assigned as the initial guess for thickness in the extraction process ($d_0 = d + U(-0.15, 0.15)$). This initial guess is chosen according to the average error between mechanical measurement of the tested samples and the extracted effective thickness. Histogram of the errors for 100 simulated cases are shown in Fig. 2 where the relative error is defined as follows:

$$\text{Relative error} = \frac{\text{exact} - \text{estimated}}{\text{exact}}. \tag{7}$$

According to Fig. 2, for 84% of the cases, the thickness and ϵ_s can be estimated with a relative error of 1% and relaxation time is extracted with a relative error of 5%. For 92% of the cases, less than ten iterations are required to obtain a fully converged result. This is an independent way to verify the accuracy of our data analysis, and it shows that the described method is reliable and rapidly converging.

3 Experimental Results

Twenty samples of $C_{36}H_{74}$ hexatriacontane, (purity: 98%, Sigma-Aldrich) with various thickness ranging from 0.3 to 2.2 mm are fabricated using casting in a metallic mold. Thickness of the samples is measured with the micrometer (Mitutoyo QuantuMike Series 293-Coolant Proof) with standard error of 0.4 μm and resolution of

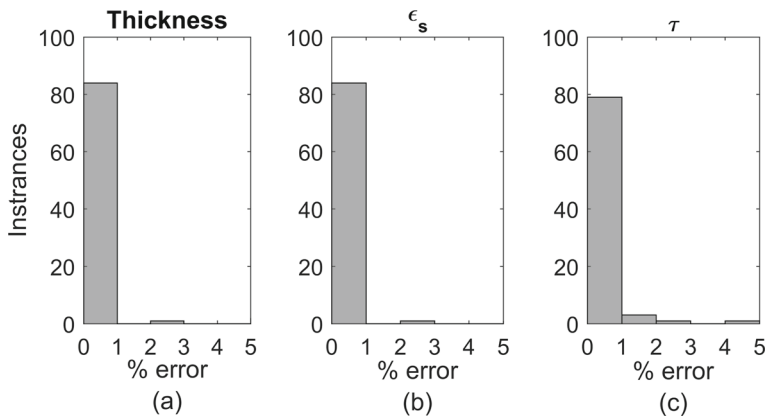

Fig. 2 Error histogram for estimated **a** thickness d, Debye relaxation parameters of **b** ϵ_s, and **c** τ

1 μm which is used as the initial guess in the least-squares fitting. Amplitude and phase of the transmitted wave through samples are measured using a commercial THz-TDS system (TPS Spectra 3000, Teraview Ltd.). Figure 1b shows the measurement chamber of the THz-TDS system. To eliminate the absorption peaks due to O_2 and water vapor, chamber is purged with N_2 throughout the measurement. First, a reference measurement is performed without the sample. Next, transmittance through the sample is measured in the frequency range of 0.06–3 THz with a frequency resolution of 734 MHz. However, only the frequency range of 0.3–1.1 THz is used for data analysis, since it has the sufficient signal-to-noise ratio. Each frequency data is averaged over 300 measurements to eliminate any random errors arising from amplitude fluctuations of the mode-locked femtosecond laser. Once the Debye relaxation parameters are determined through the least-squares optimization, complex permittivity is extracted for the frequency range of 26 GHz–1.1 THz using the procedure discussed in Section 2 and Eq. 2. Extrapolated data in the range of 26–110 GHz are of interest for the paraffin variable capacitors operating at mmW frequencies [1, 2].

As a example, temporal profile of the THz signal with and without the 1.498-mm-thick sample are shown in Fig. 3a. Transmission coefficient is calculated by the ratio of the Fourier transform of these signals. Amplitude and phase of the transmission coefficient are shown in Fig. 3b, c, respectively. As shown here, experimental data and the fitted model are in close agreement and residual sum of squares (RSS) for the amplitude and phase are 0.3243 and 0.2193, respectively.

Extraction process is performed on the 20 measured samples. The average ϵ_s and τ values are 2.2516 and 1.65 fs with standard deviation of 0.028 and 1.08 fs, respectively. Using the extracted parameters, Debye relaxation model given in Eq. 2 is used

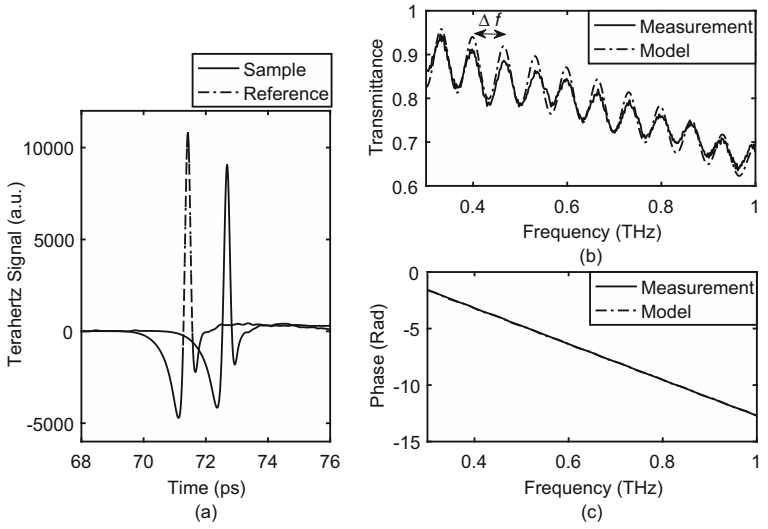

Fig. 3 **a** Measured time-domain THz pulse for the reference (without sample) and for the 1.498-mm-thick hexatriacontane sample. Comparison of the measured data with the analytical model for **b** amplitude and **c** phase of the transmittance

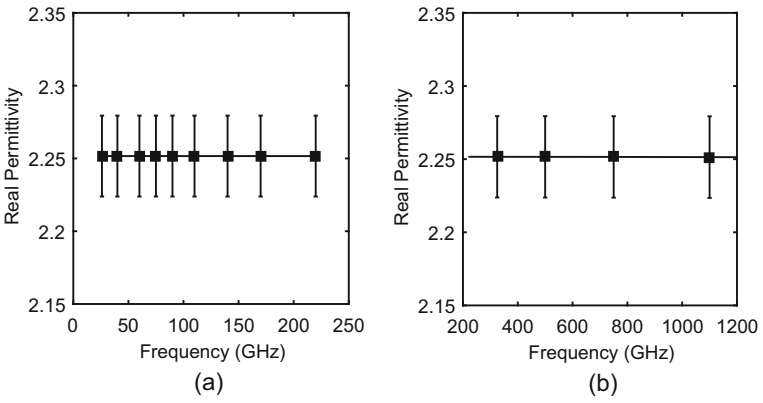

Fig. 4 **a** Measured (0.3–1.1 THz) and **b** extrapolated (26–300 GHz) average real permittivity for 20 hexatriacontane samples with error bars representing one standard deviation

to calculate the complex permittivity. Average real part of the permittivity is plotted in Fig. 4 where error bars indicate one standard deviation. Real permittivity has a average value of 2.25 with a standard deviation of 0.028, and it is approximately constant over the measured frequency range. Figure 5 shows the average loss tangent where error bars represent one standard deviation. Loss tangent is monotonically increasing with frequency and approximately has a linear dependency as follows:

$$\tan\delta = 5.7541 \times 10^{-3} f + 1.9973 \times 10^{-7} \tag{8}$$

where f is frequency in THz. As expected, uncertainties in determining the relaxation time, result in increasing standard deviation of the loss tangent with respect to frequency.

The accuracy of the extracted complex permittivity is affected by the uncertainty of the sample thickness and its roughness over the illuminated region by the THz beam. Moreover, the analytical model is no longer valid in the cases of nonparallel

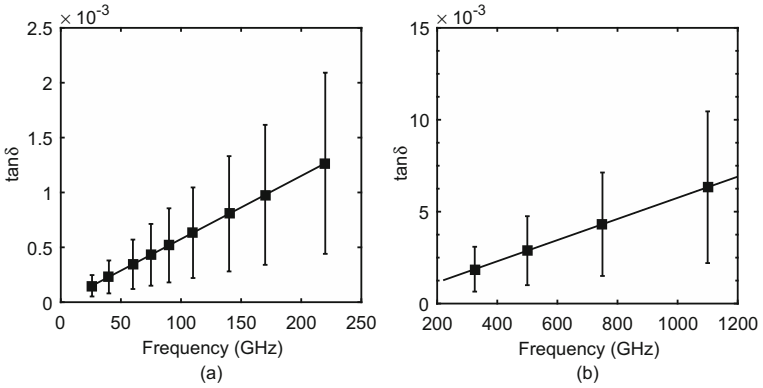

Fig. 5 **a** Extrapolated **b** measured loss tangent for 20 hexatriacontane samples for the frequency range of 26 GHz–1.1 THz. Error bars represent one standard deviation

Table 1 Average and standard deviation of loss tangent for various frequency bands

Band	Frequency	Avg. tan δ	SD
Ka	26 GHz	1.49×10^{-4}	9.75×10^{-5}
U	40 GHz	2.30×10^{-4}	1.50×10^{-4}
E	60 GHz	3.45×10^{-4}	2.25×10^{-4}
W	75 GHz	4.32×10^{-4}	2.81×10^{-4}
F	90 GHz	5.18×10^{-4}	3.37×10^{-4}
D	110 GHz	6.33×10^{-4}	4.13×10^{-4}
G	140 GHz	8.06×10^{-4}	5.25×10^{-4}
Y	170 GHz	9.78×10^{-4}	6.37×10^{-4}
–	220 GHz	1.26×10^{-3}	8.25×10^{-4}
–	325 GHz	1.87×10^{-3}	1.22×10^{-3}
–	500 GHz	2.88×10^{-3}	1.88×10^{-3}
–	750 GHz	4.31×10^{-3}	2.81×10^{-3}
–	1.1 THz	6.32×10^{-3}	4.12×10^{-3}

sample surfaces and the oblique incident of the THz beam, which results in inaccurate extracted parameters.

Summary of loss-tangent measurement results for most commonly used frequency bands is compiled in Table 1, suggesting that it can be used to design low-loss RF components in mmW and THz bands.

4 Summary and Discussion

We have reported the complex permittivity characterization method o using THz-TDS. A least-squares optimization scheme is used to fit the amplitude and phase of the transmittance to an analytical propagation model. One of the unique features of this work is that our extraction method does not require a *priori* knowledge of the thickness and temporal windowing. Accuracy of the described method is verified using Finite Element simulations and complex permittivity parameters are extracted with a relative error of less than 5 for 84% of the cases.

Using this approach complex permittivity of solid alkane samples are extracted, where Debye relaxation parameters and the thickness of the sample are simultaneously estimated. Complex permittivity for frequency range of 26–300 GHz is extrapolated. For the paraffin samples, real permittivity is measured to be 2.25 with a standard deviation of 0.028, and it is approximately constant over the frequency range of interest. Measurement results are compared with the state-of-art TDS measurements on liquid n-alkanes and solid paraffin waxes with a lower melting point (< 58 °C). Average real permittivity of hexatriacontane is higher than that of liquid n-alkanes ($C_{15}H_{32}$, $\epsilon_r = 2.04$), since the refractive index increases monotonically with respect to the number of carbon atoms [7]. Moreover, similar to refractive index of liquid n-alkanes [7] and solid paraffin waxes [8, 9], real permittivity of hexatriaconane is approximately independent of frequency in the frequency range of interest.

Measured absorption coefficient for liquid n-alkanes [7] and solid paraffin waxes [8, 9] has similar characteristics to the loss tangent of the hexatriacontane which is monotonically increasing with frequency without any absorption peaks. Although the standard deviation of the real permittivity is very low, uncertainty of the estimated loss tangent increases with frequency. Nonplanar and rough surface of paraffin contribute to the uncertainty in determination of the relaxation time which consequently increases the standard deviation of the loss tangent at higher frequencies. Extracted loss tangent values for paraffin are less than 10^{-3} for $f < 170$ GHz, and it is equal to 6.32×10^{-3} at 1.1 THz. This unique property makes alkanes an attractive material for the design of RF components and antennas in mmW and THz bands.

Funding Information This material is based upon work supported by the US National Science Foundation (NSF) under Grant No. 1408228.

References

1. B. Ghassemiparvin, S. Shah, N. Ghalichechian, in *2017 11th European Conference on Antennas and Propagation (EUCAP)* (2017), pp. 3506–3510.
2. B. Ghassemiparvin, N. Ghalichechian, in *2018 12th European Conference on Antennas and Propagation (EUCAP)* (2018).
3. K. Meng, T. nan Chen, T. Chen, L. guo Zhu, Q. Liu, Z. Li, F. Li, S. cheng Zhong, Z. ren Li, H. Feng, J. heng Zhao, Journal of Biomedical Optics **19**(7) (2014).
4. U. Stumper, Advances in Molecular Relaxation Processes **7**(3), 189 (1975).
5. N.A. Hermiz, J.B. Hasted, C. Rosenberg, Journal of the Chemical Society, Faraday Transactions 2: Molecular and Chemical Physics **78**, 147 (1982).
6. W. Richter, D. Schiel, Infrared Physics **24**(2), 227 (1984).
7. J.P. Laib, D.M. Mittleman, Journal of Infrared, Millimeter, and Terahertz Waves **31**(9), 1015 (2010).
8. L. Tian, X. Xu, Journal of Infrared, Millimeter, and Terahertz Waves **39**(3), 302 (2018).
9. X.S. Kang, P.J. Huang, X. Li, D.B. Hou, J.H. Cai, G.X. Zhang, **602**, 2675 (2014).
10. B. Ghassemiparvin, N. Ghalichechian, in *2016 International Workshop on Antenna Technology (iWAT)* (2016), pp. 48–50.
11. B. Ghassemiparvin, N. Ghalichechian, in *2017 IEEE International Symposium on Antennas and Propagation USNC/URSI National Radio Science Meeting* (2017), pp. 887–888.
12. L. Duvillaret, F. Garet, J.L. Coutaz, IEEE Journal of Selected Topics in Quantum Electronics **2**(3), 739 (1996).
13. L. Duvillaret, F. Garet, J.L. Coutaz, Applied Optics **38**(2), 409 (1999).
14. T.D. Dorney, R.G. Baraniuk, D.M. Mittleman, Journal of Optical Society of America. A **18**(7), 1562 (2001).
15. I. Pupeza, R. Wilk, M. Koch, Opt. Express **15**(7), 4335 (2007).
16. J. Sun, S. Lucyszyn, IEEE Access **6**, 8302 (2018).
17. W.C. Chew, *Waves and fields in inhomogeneous media* (IEEE press, 1995).